LONGSHORE SAND TRANSPORT CALCULATED BY TIME-DEPENDENT SHEAR STRESS

Ernest R. Smith[1] and Nicholas C. Kraus[1]

1. U.S. Army Engineer Research and Development Center, Coastal and Hydraulics Laboratory, 3909 Halls Ferry Road, Vicksburg, MS 39180-6199, USA. Ernest.R.Smith@erdc.usace.army.mil; Nicholas.C.Kraus@erdc.usace.army.mil.

Abstract: Based on longshore sand transport experiments performed in a large basin, measured sand transport rates obtained for spilling and plunging waves are compared to the Bodge and Dean (1987) and Watanabe (1992) distributed load formulas, representative of typical formulas applied in engineering practice. Neither formula estimates the measurements satisfactorily. The Bodge and Dean formula is sensitive to changes in energy flux and does not include threshold shear. The Watanabe formula includes critical shear, but transport estimates are made from time-averaged values of bottom shear stress, which did not exceed critical shear stress at most cross-shore locations. A new transport formula is introduced based on time-dependent shear stress calculated from the total velocity that includes the wave orbital velocity. The new formula gives reasonable estimates for both spilling and plunging breaker types. A conclusion is that it is essential to represent the time-dependent, or fluctuating, component of fluid motion in predictive equations of the longshore sand transport rate.

INTRODUCTION

Many studies have been conducted to relate longshore sand transport rates to wave and current processes for developing predictive capability in terms of variables that are relatively easy to measure or hindcast. Total, or bulk, load transport refers to the total amount of sand transported along the coast in the surf zone. Distributed transport refers to the cross-shore distribution of longshore transport with a varying local rate across the surf zone. Despite the many studies that have been performed worldwide to develop accurate estimates for the longshore sand transport rate, there are limitations for quantitative applications. The purpose of this paper is to compare the existing distributed

load models of Bodge and Dean (1987) and Watanabe (1992) to high quality mid-scale laboratory data, and to introduce a new distributed load model based on the time-dependent shear stress that more reliably reproduces the measurements.

LABORATORY EXPERIMENTS

Mid-scale laboratory experiments were performed to measure the longshore sand transport and nearshore hydrodynamics in a controlled environment. Mid-scale denotes wave and current conditions that commonly occur on coasts such as the Gulf of Mexico and the Great Lakes. "Midscale" contrasts with much smaller wave heights and shorter wave periods typically generated in three-dimensional laboratory basin facilities. For example, mid-scale wave height and period might be on order of 0.25 m and 3 sec, respectively, as opposed to small-scale laboratory conditions on the order of 0.1 m and 1 sec. Because wave energy is proportional to the square of wave height and energy flux to the 5/2 power of wave height, more than doubling the wave height capable in mid-scale experiments as compared to traditional small-scale laboratory experiments greatly increases mean energy and associated turbulence in the surf zone. Longer wave period increases the extent of the area considered as shallow water.

Numerous laboratory and field studies have found that suspended sand concentration at the breaker line is strongly influenced by breaker type. Sand concentrations measured under plunging breakers are significantly greater than concentrations measured under spilling breakers of similar wave height (Kana 1977; Wang et al. 2002). Because longshore sand flux is the product of sand concentration and longshore current velocity, greater concentration would result in greater sand transport given similar longshore current velocity. The laboratory experiments were designed to include both spilling and plunging breaker types.

LSTF Facility and Experiment Design

The Longshore Sediment Transport Facility (LSTF) is a large-scale laboratory facility capable of simulating conditions comparable to low-wave energy coasts. The sand beach consists of 150 m^3 of fine quartz sand having a mean diameter d_{50} of 0.15 mm. An external recirculation system can maintain a steady and uniform wave-generated longshore current along the beach to minimize boundary effects. The LSTF includes instruments to measure water surface elevation, 3-D current velocity, and sand concentration simultaneously at several cross-shore locations. Wave gauges and acoustic Doppler velocimeters (ADV's) are mounted on a movable bridge that can be positioned at any location along the shore. Twenty sand traps at the downstream boundary of the model are instrumented with load cells to weigh trapped sand and are used to measure total cross-shore distribution of the total longshore sand transport rate generated under obliquely incident waves. Hamilton et al. (2001) discuss LSTF features and capabilities.

Four irregular wave signals with relatively broad spectral shape representative of sea conditions were generated in these LSTF tests. They were designed to obtain and compare transport rates for different breaker types through varying incident wave height and period. Four conditions generated in the LSTF are listed in Table 1, where H_{mo} is

energy-based significant wave height measured near the wave generators, H_{mob} is wave height at breaking, T_p is peak wave period, h is water depth at the wave generators, θ_b is incident wave angle at the generators, and m is the average slope of the beach from the breaker line to the shoreline. The wave conditions can be grouped by energy level. Tests 1 and 3 had similar incident wave height and are referred to as higher energy conditions, and Tests 5 and 6 are referred to as lower energy conditions. Each test was conducted with an h = 0.9 m and θ = 10 deg at the wave generators.

Table 1. LSTF test wave conditions

Test Number	Breaker Type	H_{mo} m	H_{mob} m	T_p sec	h m	θ_b deg
1	Spilling	0.25	0.26	1.5	0.9	6.5
3	Plunging	0.23	0.27	3.0	0.9	6.4
5	Spilling	0.16	0.18	1.5	0.9	6.7
6	Plunging	0.19	0.21	3.0	0.9	6.4

LSTF Results

The cross-shore distribution of wave height of each test is shown in Fig. 1. Test 3 and Test 6 waves shoaled prior to breaking and decreased in height sharply directly shoreward of breaking, typical of plunging waves. Test 1, a spilling case, also showed a sharp decrease in height directly shoreward of breaking. Test 1 had a surf similarity parameter on the upper end of spilling waves, 0.34 (Smith and Kraus 1991), and some plunging waves were observed within the time series; however, waves were observed to break predominately by spilling. Wave height in Test 5 decayed through the surf zone, typical of spilling breakers.

Measured longshore sand flux is plotted as a function of cross-shore location in Fig. 2. Three distinct zones of transport are evident; the incipient breaking zone, inner surf zone, and swash zone. At incipient breaking, a substantial peak in transport occurs for the plunging-waves (Tests 3 and 6), but is not observed in the spilling-waves (Tests 1 and 5). Shoreward of breaking, in the inner surf, wave energy is saturated, and wave height is strongly controlled by depth, independent of wave period. Fig. 2 implies that longshore sand flux in the inner surf zone is dominated by wave height, independent of period. A peak in transport occurs in the swash zone for all tests. For waves having similar incident wave height, but different period, i.e., Tests 1 and 3, and Tests 5 and 6, swash zone transport is much greater for the longer period tests. This result is consistent with elevation of wave runup (Hunt 1959), in which runup is directly proportional to wave period.

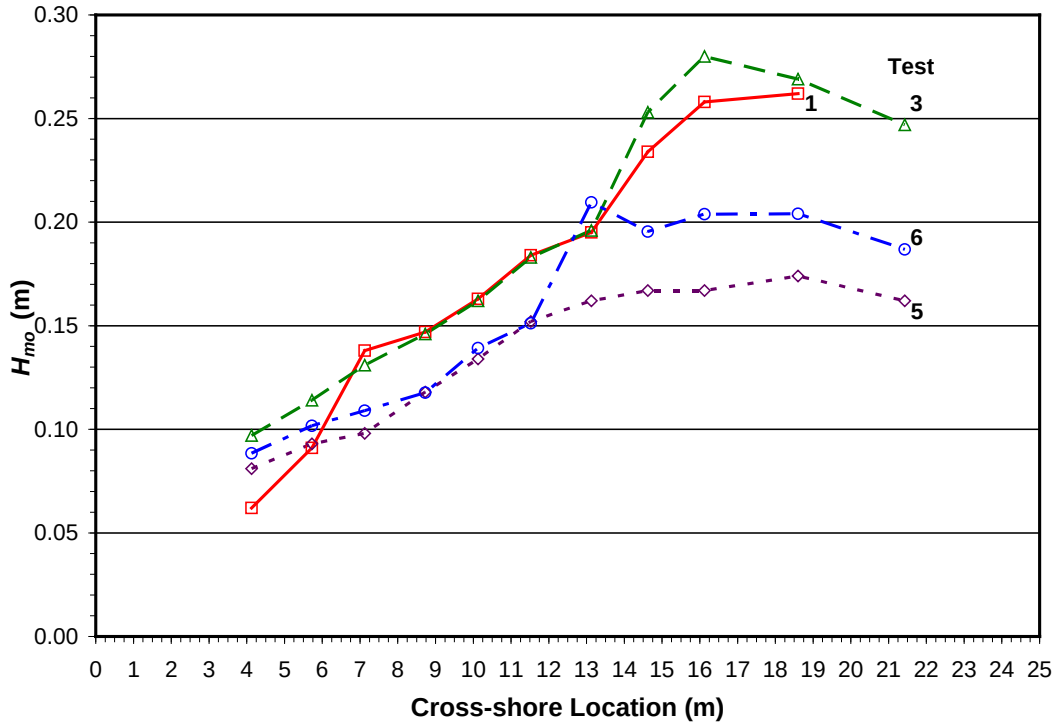

Fig. 1. Cross-shore distribution of measured wave height

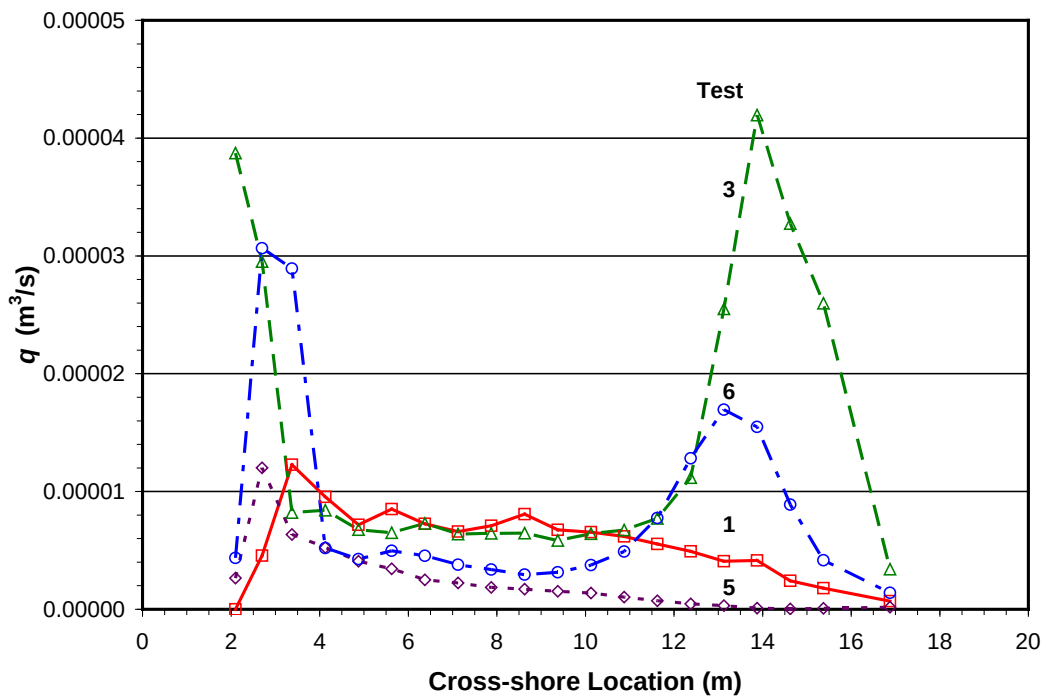

Fig. 2. Cross-shore distribution of measured longshore sand flux

COMPARISON OF LSTF DATA TO SELECTED PREDICTIVE FORMULAS

Smith et al. (2006) compared LSTF results to distributed load formulas of Bodge and Dean (1987) (B&D) and Watanabe (1992), summarized here. B&D examined forms of energetics and stress models and developed several alternative formulas based on laboratory experiments and short-term impoundment of sand under moderate wave conditions in the field. The recommended equation from their study, which predicts longshore transport based on wave energy dissipation and is valid only inside the surf zone where wave energy is expected to dissipate by depth-limited breaking, is given as:

$$i_y = \frac{k_q}{h}\frac{\partial F}{\partial x} V \left[\frac{dh}{dx}\right]^r \tag{1}$$

where i_y is the local immersed weight sand transport rate (force/time) per unit offshore length, k_q is a dimensional coefficient found equal to 0.057 sec for laboratory data and 0.48 sec for field data, h is local water depth, x is cross-shore position, F is average wave energy flux per unit surface area, V is the mean local longshore current, and r is a dimensionless constant, where r = 0.5 gave the best agreement with the B&D data set. However, Bodge (1989) stated that scaling effects in the B&D movable-bed laboratory experiments may have exaggerated the apparent relationship between local transport and bottom slope, and that r may equal 0, eliminating the last factor of Eq. 1. In shallow water, average wave energy flux per unit surface area in linear wave theory is the product of wave energy per unit surface area, E, and wave group celerity, C_g:

$$F = EC_g = \left(\frac{\rho g H^2}{8}\right)\sqrt{gh} \tag{2}$$

where ρ is fluid density, g is acceleration due to gravity, and H is local wave height.

Fig. 3 shows that the B&D formula follows the general trend of the Test 1 measurements and predictions vary greatly for the spilling wave condition. Test 3 measurements were underestimated and no transport is calculated in the trough of the breakpoint bar, because dh/dx is negative. The model is based on energy dissipated and will not predict transport where no dissipation theoretically occurs, i.e., regions of increasing wave height or increasing depth, such as from a bar crest to bar trough. Wave gauges were not located in the swash zone, so transport estimates in the swash zone could not be made.

The B&D formula with r = 0 is compared to the LSTF measurements in Fig. 4. The B&D formula significantly over-predicts Test 1 measurements. Dropping the slope term produced a transport estimate near the Test 3 breakpoint, but the model greatly over-predicted transport shoreward of breaking. Estimates can be improved by adjusting k_q, but a different coefficient would be required to give optimal results for each breaker type.

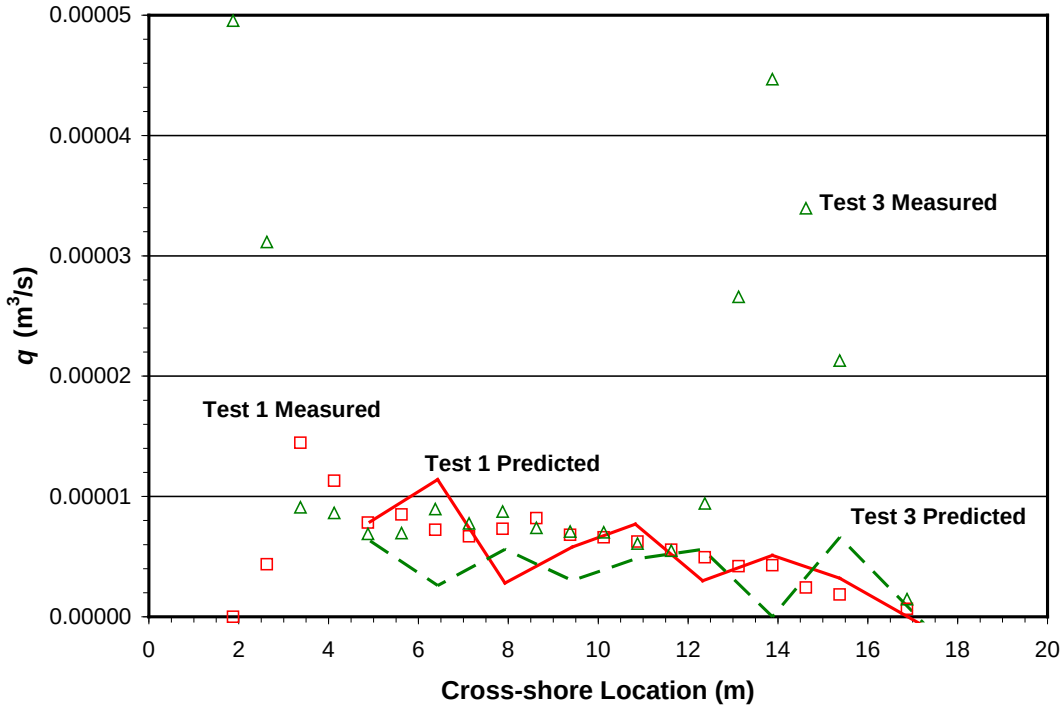

Fig. 3. Bodge and Dean (1987) estimates compared to Test 1 and Test 3 (r = 0.5)

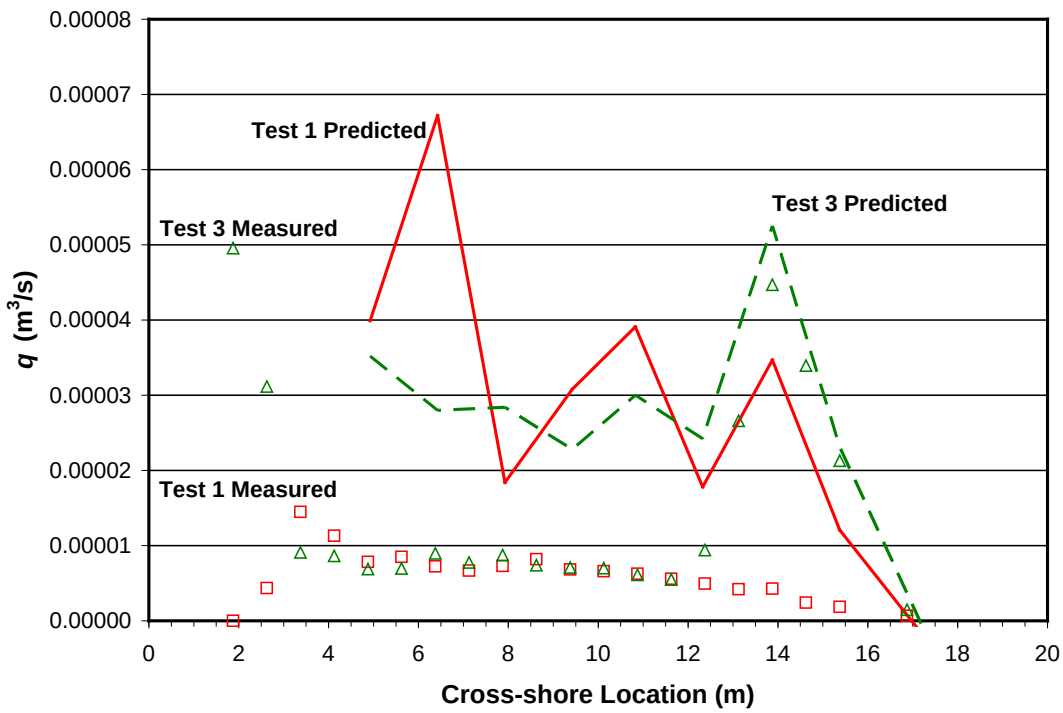

Fig. 4. Bodge and Dean (1987) estimates compared to Test 1 and Test 3 (r = 0)

Watanabe (1992) (W92) proposed a Meyer-Peter and Muller-type equation to calculate longshore sand transport as combined bed and suspended load of the form:

$$q_y = A\left[\frac{(\tau - \tau_{cr})V}{\rho g}\right] \tag{3}$$

where τ_{cr} is the critical shear stress for inception of sediment motion, and A is an empirical coefficient approximately equal to 2 for irregular waves. The magnitude of the total bottom shear stress under waves and currents is represented here as:

$$\tau = \frac{\rho c_f}{2}\sqrt{U^4 + V^4} \tag{4}$$

in which c_f is the bottom friction coefficient for combined waves and quasi-steady current and was calculated as in Buttolph et al. (2006), and U and V are the mean cross-shore and longshore velocities, respectively. Critical shear stress is calculated as:

$$\tau_{cr} = (\rho_s - \rho_w)\, g d_{50} \theta_{cr} \tag{5}$$

where ρ_s is the density of the sediment, d_{50} is expressed in meters, and θ_{cr} is the critical Shields parameter for sediment motion, taken to be 0.05 for 0.15-mm diameter sand.

The difference in shear stresses in Eq. 3 can be interpreted as representing a stirring function, and the velocity term represents a transport function. This formula has received wide-spread application for its simplicity, while incorporating several physical processes.

The W92 formula is applied to the LSTF Tests 1 and 3 (Fig. 5). Transport is not predicted at several cross-shore locations for both the plunging and spilling breaker conditions because the time-averaged bottom shear stress did not exceed the critical shear at those locations. The formula fails for low-wave conditions because it only estimates transport where the time-averaged bottom shear stress exceeds the critical shear, true for virtually all the smaller wave test locations (Tests 5 and 6).

The two predictive formulas evaluated did not perform well in comparisons to high-quality LSTF data. The B&D model either greatly underestimated the transport at the plunging wave breakpoint or over estimated the spilling wave case, depending on whether the slope term was included. The formula was sensitive to changes in energy flux, and it does not include threshold shear or differentiate between breaker types. The W92 formula includes threshold shear, but estimates longshore sand transport from only the time-averaged values of current. The time-averaged bottom shear stress exceeded critical shear stress at only a few cross-shore locations in the laboratory. Additionally, breaker type is not represented, nor is the wave orbital velocity in the surf zone. These results motivated examination of sand transport mechanics from a more basic approach.

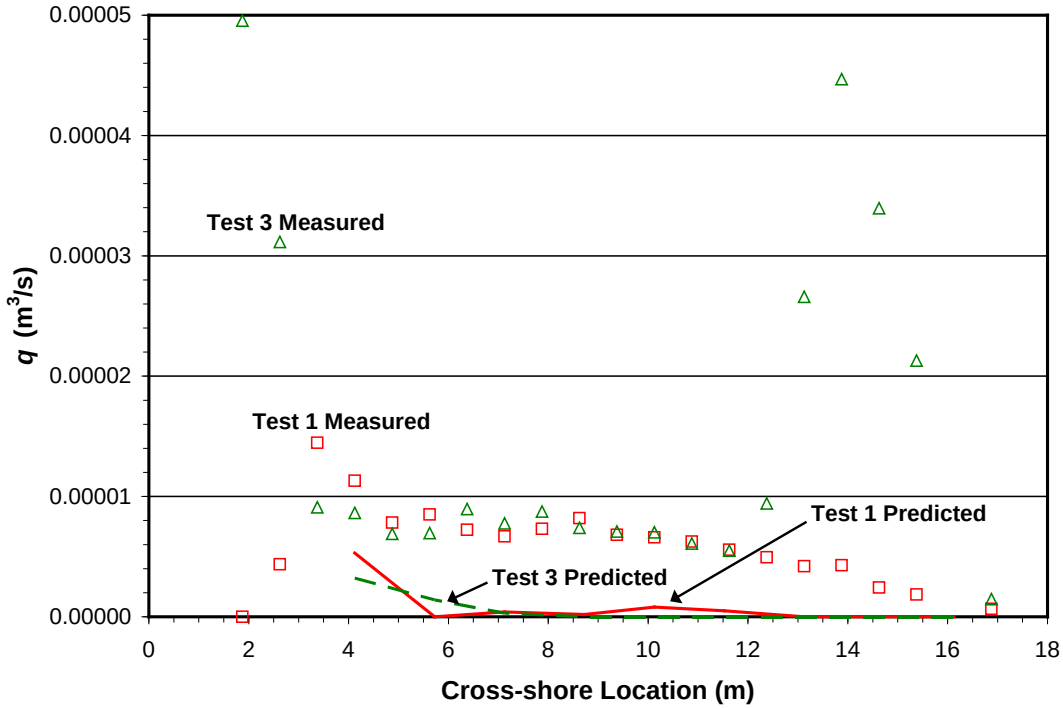

Fig. 5. Watanabe (1992) estimates compared to Test 1 and Test 3

PREDICTIVE FORMULA BASED ON TIME-DEPENDENT SHEAR STRESS

Madsen (1991) states that any model of sediment response to fluid forces that relies on the mean turbulent flow characteristics is limited to being conceptual. The necessity of including the fluctuating component of fluid motion was motivated by the findings of Madsen and Grant (1976), who noted that a sediment grain at point of incipient motion reacts to the fluctuations rather than to the mean value of the entraining force. Kraus et al. (1988) demonstrate that trends in prediction of the local longshore sand transport rate in the surf zone is improved by including the dissipation of waves and standard deviation in the longshore current velocity, both of which represent variations in fluid motion.

The shear stress, including the fluctuating component together with the mean value, can be calculated from the wave orbital velocity measured with the ADV's installed in the LSTF. The total cross-shore component of velocity is written:

$$u(t) = U + u'(t) \tag{6}$$

where U is the time-mean of $u(t)$, and $u'(t)$ is the fluctuating component that includes wave orbital velocity and turbulence. Similarly, the total longshore current velocity can be written as:

$$v(t) = V + v'(t) \tag{7}$$

where V is the time mean of $v(t)$, and $v'(t)$ is the fluctuating component and is typically small compared to V. The total shear stress exerted by the water on the sand bottom is:

$$\vec{\tau}(t) = \hat{x}\,\tau_x + \hat{y}\,\tau_y \tag{8}$$

the magnitude of which is:

$$\tau(t) = \sqrt{\tau_x(t)^2 + \tau_y(t)^2} = \frac{\rho_w c_f}{2}\sqrt{u(t)^4 + v(t)^4} \tag{9}$$

The time series of τ was calculated via Eq. 9 for Test 1, spilling waves at four ADV's having cross-shore locations X = 18.6, 13.1, 8.7, and 4.1 m (Fig. 6). At the most offshore ADV (X = 18.6 m), shear stress sometimes exceeded $\tau_{cr,}$ but often did not (Fig. 6a). This result indicates that the sand in the LSTF for this location was only occasionally mobilized for transport, so the transport rate is expected to be small. The magnitudes of total shear stress were much greater at ADV's located at X = 13.1 m and X = 8.7 m (Figs. 6b and 6c, respectively), and transport rates are expected to be greater at these cross-shore locations. Fig. 6d shows that shear stress magnitudes decrease at the most onshore ADV located at X = 4.1 m, but τ_{cr} was exceeded more frequently, i.e., sand was mobilized for transport more frequently at the most onshore ADV than at the other locations shown. The greater mobilization calculated correlates to the cross-shore distribution of sand transport rate observed for this case (Fig. 2).

The original W92 formula (Eq. 3) includes only the mean shear stress and predicted no transport at many LSTF cross-shore locations because the shear stress based on mean velocity did not exceed the critical shear (Fig. 5). In contrast, Fig. 6 shows that the total velocity components, which include the fluctuating components *u'* and *v'*, produce a shear stress that frequently exceeds the critical shear. Therefore, accounting for the fluctuating component is essential for reproducing longshore sand transport under different types of breaking waves for smaller wave conditions.

Several transport formulas were investigated in this study based on the concept of:

$$q(t) \;=\; ST(t) \;\times\; TR(t) \tag{10}$$

where $q(t)$ is the time-dependent transport rate per unit length perpendicular to the transport, ST is a stirring function that mobilizes the sand, and TR is a transporting function that moves the sediment (Kraus and Horikawa 1990).

Equation 10 must be averaged over the time record, with the average taken of the full expression, although the averages of each factor on the right-hand side may be of interest in examining the physical processes of sand stirring and transport. A new formula was developed based on the time-mean of longshore sand transport rate:

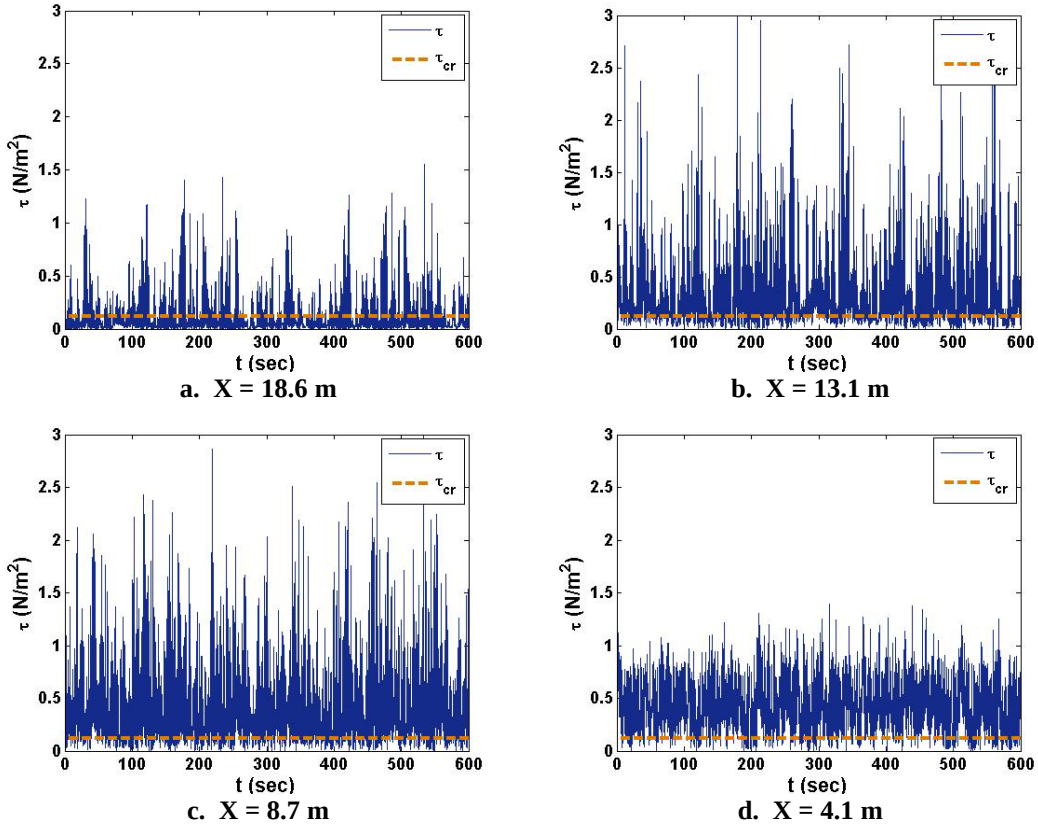

Fig. 6. Time history of $\boldsymbol{\tau}$

$$q_y = K\left\langle \left(ST(t) - \tau_{cr}\right)\left(TR_y(t)\right)\right\rangle \tag{11}$$

where K is an empirical parameter that may involve several dimensional quantities, depending on the stirring function $ST(t)$ and transporting function $TR_y(t)$, and <-> represents the time-average operation.

The stirring function $ST(t)$ is the time-average of τ:

$$\langle ST \rangle = \langle \tau(t) \rangle = \frac{1}{N}\sum_{1}^{N} \tau(t) \tag{12}$$

where N is the number of calculation points. For calculating the longshore transport rate, the transporting function $TR_y(t)$ is $v(t)$, Eq. 7, and the time-average is V.

It was observed during the LSTF plunging wave experiments that sand remained in suspension at the trough of the break-point bar for the duration of the tests. The plunging waves distributed sand through the water column, and sand entrained in the upper water column had a greater distance to settle to the bed, requiring a time interval longer than several wave periods. Subsequent waves would redistribute the suspended sand through

the water column. Therefore, sand entrained into the water column by a single plunging wave would continue to be transported during several subsequent waves. An additional term to account for events that cause sand to be suspended through the water column and increase the transport rate near the break point of plunging waves is included in the model. This suspension term $s(t)$ is as defined as:

$$s(t) = \left(u'(t)^2 + v'(t)^2\right)^k \tag{13}$$

where k is an empirical exponent set to 2 based on numerical comparison to the LSTF data.

The new predictive longshore sand transport rate formula based on time-dependent shear stress is then given as:

$$\begin{gathered} q_y(t) = \left(f_b K\left(\tau(t) - \tau_{cr}\right) + f_s s(t)\right)V \quad \text{for } \tau(t) > \tau_{cr} \\ \text{and} \\ q_y(t) = 0 \quad \text{for } \tau(t) < \tau_{cr} \end{gathered} \tag{14}$$

where f_b = 10 and f_s = 0.014 are empirical coefficients determined by comparisons to the LSTF results. The time-averaged transport rate over the record was calculated by:

$$q_y = \frac{1}{N}\sum_{1}^{N} q_y(t) \tag{15}$$

Estimates of Test 1 longshore sand transport rates were improved using the time dependent formula (Eq. 15), as shown in Fig. 7. The equation modeled the trend and general magnitude of measured transport rates. Transport rates for Test 3 also are estimated well, especially near breaking and in the surf zone onshore of X = 6 m.

The time-dependent formula was compared to the smaller waves of Test 5 and Test 6 (Fig. 8). Estimates followed the trend of the measured distribution, although slightly high, and were good onshore of X = 6 m. Estimates with Test 6 conditions gave good agreement with measurements. Eq. 15 predicts a peak in transport near breaking with Test 6 waves, although lower than measured, and estimates surf zone transport rates well.

The same values of the empirical coefficients were used for all LSTF test conditions. Eq. 15 estimated the trend and magnitude of cross-shore distributed longshore sand transport rates for both spilling and plunging breakers. Although ADV's were not present throughout the swash zone, the formula presented is capable of estimating swash zone transport if the swash zone hydrodynamics are available for input.

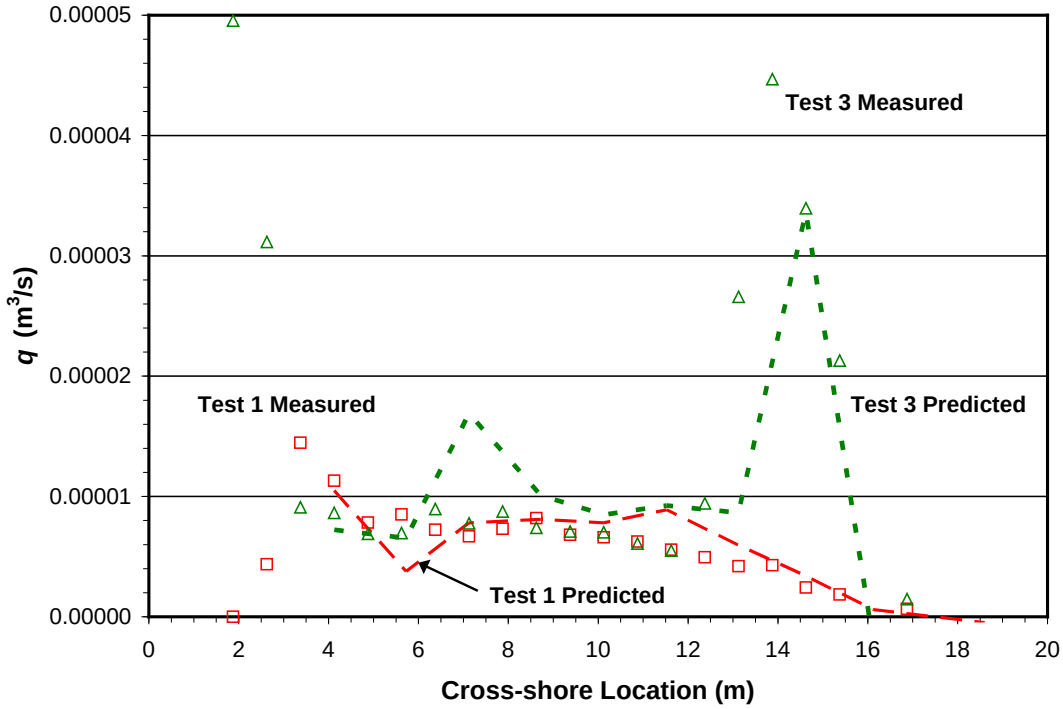

Fig. 7. Estimated transport rate from time-dependent shear stress model, Tests 1 and 3

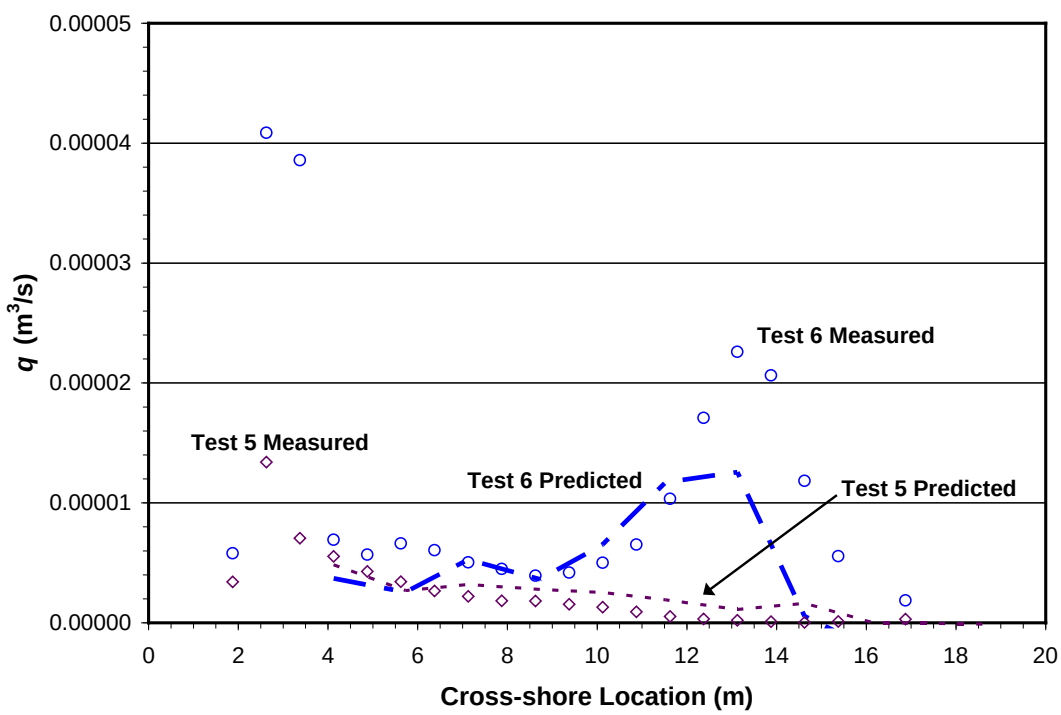

Fig. 8. Estimated transport rate from time-dependent shear stress model, Tests 5 and 6

CONCLUDING DISCUSSION

A key finding of the present study is that it is essential to include the fluctuating component of the wave orbital velocity in predictive sand transport rate equations for the surf zone. Bottom shear stress calculated from the mean velocity rarely exceeds the critical shear for sand motion for small waves or for sediment with a large grain size. Figure 5 illustrates that the original Watanabe (1992) equation, which is based on mean bottom shear stress, predicts zero sand transport for several of the LSTF cross-shore locations. Also, mean values of the longshore current and cross-shore current do not contain significant information on the wave breaking process, which determine in great part the intensity and vertical extent of fluctuations produced. Therefore, it is concluded that the fluctuating component of shear stress must be included in future hydrodynamic simulations aimed at providing forcing for calculating longshore sand transport.

Additionally, breaker type was found to be a central variable in the amount of sand transport that occurs at a location, which agrees with the findings of Kana 1977 and Wang et al. 2002. Plunging breakers produce greater turbulence throughout the water column whereas turbulence associated with spilling breakers remains near the surface in the bore. Mean values of the longshore and cross-shore current do not provide information on the wave breaking process, which determines the amount of turbulence produced.

A new formula was developed that yielded improved estimates of longshore sand transport and includes the fluctuating component of wave orbital velocity. For engineering purposes, the fluctuating component can be related to the mean wave orbital velocity, which is a function of wave height and period. As a result, an accurate wave transformation model is necessary to give reliable estimates of distributed longshore sand transport rates. Comparison of the new predictive transport formula and field measurements is underway, the results are so far favorable.

ACKNOWLEDGEMENTS

The authors wish to acknowledge William Halford, David Daily, and Tim Nisley who provided technical support during the experiments. Data collection presented in this paper was supported by the Navigation System Research Program, U.S. Army Corps of Engineers (USACE). Writing of this paper was supported by the Coastal Inlets Research Program, USACE. Permission to publish this information was granted by Headquarters, USACE.

REFERENCES

Bodge, K.R. (1989). “A literature review of the distribution of longshore sediment transport across the surf zone,” *J. Coastal Res.* 5(2), 307-328.

Bodge, K.R., and Dean, R.G. (1987). “Short-term impoundment of longshore transport,” *Proc. Coastal Sediments '87*, 468-483.

Buttolph, A.M., Reed, C.W., Kraus, N.C., Ono, N., Larson, M., Camenen, B., Hansen, H., Wamsley, T.V., and Zundel, A.K. (2006). "Two-dimensional depth-averaged circulation model CMS-M2D: Version 3.0, Report 2, sediment transport and morphology change," ERDC/CHL-TR-06-9, U.S. Army Engineer Research and Development Center, Vicksburg, MS.

Hamilton, D.G., Ebersole, B.A., Smith, E.R., and Wang, P. (2001). "Development of a large-scale laboratory facility for sediment transport study." TR ERDC/CHL TR-01-22, U.S. Army Engineer Waterways Experiment Station, Vicksburg, MS.

Hunt, I.A. (1959). "Design of seawalls and breakwaters." *J. Waterways and Harbors Division*, ASCE, 85(WW3), 123-152.

Kana, T.K. (1977). "Suspended sediment transport at Price Inlet, S.C.," *Proc. Coastal Sediments '77*, 366-382.

Kraus, N.C., Gingerich, K.J., and Rosati, J.D. (1988). "Toward an improved empirical formula for longshore sand transport." *Proc. 21st Coastal Eng. Conf.*, ASCE, 1183-1196.

Kraus, N.C., and Horikawa, K. (1990). "Nearshore sediment transport." in *The sea, ocean engineering science*, part B, B. LeMehaute and D.M. Hanes (eds.), John Wiley and Sons, 775-813.

Madsen, O.S. (1991). "Mechanics of cohesionless sediment transport in coastal waters," *Proc. Coastal Sediments '91*, 15-27.

Madsen, O.S., and Grant, W.D. (1976). "Quantitative description of sediment transport by waves." *Proc. 15th Coastal Eng. Conf.*, ASCE, 1093-1112.

Smith, E.R., and Kraus, N.C. (1991). "Laboratory study of breaking waves on bars and artificial reefs." *J. Waterway, Port, Coastal and Ocean Eng.*, 117(4), 307-325.

Smith, E.R., Zhang, J., and Wang, P. (2006). "Longshore sediment transport research performed in a large-scale basin," *Proc. First Int'l Conf. on Application of Physical Modelling to Port and Coastal Protection*, in press.

Wang, P., Smith, E.R., and Ebersole, B.A. (2002). "Large-scale laboratory measurements of longshore sediment transport under spilling and plunging breakers," *J. Coastal Res.*, 18, 118-135.

Watanabe, A. (1992). "Total rate and distribution of longshore sand transport." *Proc. 23rd Coastal Eng. Conf.*, ASCE, 2528-2541.